

A Climatology and Comparison of Parameters for Significant Tornado Events in the United States

JEREMY S. GRAMS AND RICHARD L. THOMPSON

NOAA/NWS/Storm Prediction Center, Norman, Oklahoma

DARREN V. SNIVELY

Department of Geography, Ohio University, Athens, Ohio

JAYSON A. PRENTICE

Department of Geological and Atmospheric Sciences, Iowa State University, Ames, Iowa

GINA M. HODGES AND LARISSA J. REAMES

School of Meteorology, University of Oklahoma, Norman, Oklahoma

(Manuscript received 18 January 2011, in final form 30 August 2011)

ABSTRACT

A sample of 448 significant tornado events was collected, representing a population of 1072 individual tornadoes across the contiguous United States from 2000 to 2008. Classification of convective mode was assessed from radar mosaics for each event with the majority classified as discrete cells compared to quasi-linear convective systems and clusters. These events were further stratified by season and region and compared with a null-tornado database of 911 significant hail and wind events that occurred without nearby tornadoes. These comparisons involved 1) environmental variables that have been used through the past 25–50 yr as part of the approach to tornado forecasting, 2) recent sounding-based parameter evaluations, and 3) convective mode. The results show that composite and kinematic parameters (whether at standard pressure levels or sounding derived), along with convective mode, provide greater discrimination than thermodynamic parameters between significant tornado versus either significant hail or wind events that occurred in the absence of nearby tornadoes.

1. Introduction

Severe weather forecasting has evolved considerably since the formation of the Severe Local Storms (SELS) Center of the U.S. Weather Bureau in the early 1950s (Corfidi 1999), to the current variation of SELS known as the Storm Prediction Center (SPC). Forecasting in the early days of SELS was limited largely to pattern recognition, sounding analysis, and subjectively predicting changes in the convective environment (Schaefer 1986; Galway 1992). Advances in numerical modeling and detailed field observations have resulted in a greater physical understanding of the processes supportive of

severe thunderstorms and tornadoes (e.g., Bluestein 1999; Davies-Jones et al. 2001; Wilhelmson and Wicker 2001). This increasing knowledge base has manifested itself in a more ingredients-based approach (Doswell et al. 1996) to severe storm forecasting—focusing on parameters representing relevant physical processes (Johns and Doswell 1992; Moller 2001), and also leading to numerous observational studies aimed at identifying environmental characteristics associated with various types of severe thunderstorms and tornadoes (e.g., Johns et al. 1993; Rasmussen and Blanchard 1998; Thompson et al. 2003).

Operational meteorologists have benefited from a dramatic increase in the quantity and quality of numerical weather prediction model guidance since the mid-1990s with the advent of gridded model output and numerous sounding-derived parameters related to severe storm occurrence (e.g., measures of buoyancy and vertical wind

Corresponding author address: Jeremy S. Grams, Storm Prediction Center, Ste. 2300, 120 David L. Boren Blvd., Norman, OK 73072.
E-mail: jeremy.grams@noaa.gov

shear). This has largely supplanted basic pattern recognition techniques, further confirmed by recent studies such as that of Bunkers et al. (2010), which discouraged the exclusive use of 700-hPa temperatures to assess the degree of capping inversion associated with an elevated mixed layer (EML). Nevertheless, mandatory pressure-level displays are commonly utilized by operational meteorologists, and it is these fields that form the initial basis of many significant tornado forecasts at the SPC. Gridded depictions of base-state variables (e.g., winds, heights, temperatures, dewpoints) allow SPC forecasters to quickly quantify and/or infer degrees of moisture, instability, and lift, prior to more vigorous interrogation of sounding-derived measures. This is especially true for the timely production of convective outlooks since several mandatory-level variables are relevant proxies to a corresponding sounding-derived evaluation (e.g., 850- and 500-hPa wind direction and speed for low- and midlevel shear; temperatures and dewpoints for instability and buoyancy). In addition, parameterized convective processes present in operational model forecast soundings substantially modify thermodynamic profiles and associated parameters in ways that can be difficult to correlate to observed physical processes (Kain et al. 2003). Thus, the use of mandatory pressure-level winds, heights, temperatures, and dewpoints (including their changes within an Eulerian frame of reference) remains an integral part of the analysis and forecast process at the SPC.

Miller (1972) noted several mandatory pressure-level and surface parameters associated with significant severe weather outbreaks. In general, indicators for outbreak events were characterized by stronger tropospheric flow, greater instability and low-level moisture, and greater midlevel height and surface pressure falls, compared to nonoutbreak severe events. However, significant tornado outbreaks are sometimes associated with weak or ill-defined forcing (e.g., Thompson and Edwards 2000), which has been shown to favor discrete cell development (Schumann and Roebber 2010). Conversely, strong forcing tends to favor mixed or linear convective modes (e.g., Bunkers et al. 2006; Dial et al. 2010). Given this, along with the operational use of simulated radar reflectivity from convection-allowing model guidance (Kain et al. 2008), convective mode is an important consideration in forecasting significant severe storm events (e.g., Thompson and Mead 2006) based on radar identification of the primary storm types associated with such events.

Trapp et al. (2005) examined all reported tornadoes from January 1998 through December 2000 and the associated radar reflectivity mosaics to establish the relative frequency of tornadoes with quasi-linear convective

systems (QLCSs). Their results suggest that QLCSs are responsible for as much as 35%–50% of all tornadoes in the Midwest (e.g., Indiana and surrounding states), and that QLCS tornadoes occasionally produce damage rated as category 2–4 on the enhanced Fujita scale (EF2–EF4¹). Gallus et al. (2008) and Duda and Gallus (2010) examined all reported severe weather events over a 10-state region from most of the Great Plains to the upper and middle Mississippi River valley during the period of 1 April–31 August in 2002 and 2007, respectively. Their results suggest that around 35% of all severe reports were associated with QLCSs. However, operational meteorologists at the SPC, as well as long-time storm enthusiasts, have noted a distinct tendency for significant tornadoes (EF2–EF5 damage) in the Great Plains to occur with discrete supercells as opposed to linear convective systems.

The goals of this work are to 1) provide a national, several-year-long climatology of convective mode for significant tornado events and 2) compare convective mode to mandatory-level kinematic–thermodynamic variables and their associated sounding-derived measures to calibrate forecaster observations and preferences when attempting to forecast significant tornado events. To achieve these goals, we documented all significant tornadoes across the contiguous United States (CONUS) from 2000 to 2008, and assigned a radar-based convective mode to each tornado. Environmental variables that have been used through the past 25–50 yr as part of the pattern recognition approach to tornado forecasting were cataloged for each tornado event, and these variables were compared to more recent sounding-based parameter evaluations (e.g., Rasmussen and Blanchard 1998; Rasmussen 2003; Thompson et al. 2003) for each event. The same information was collected for a comparison dataset of significant severe thunderstorm events that occurred without tornadoes. Finally, a statistical comparison was performed to determine which of the mandatory-level variables, sounding-based parameters, and convective modes provide better discrimination between significant tornado events and significant severe thunderstorm events that occurred without tornadoes.

2. Data and methods

a. Event selection

Two distinct databases of severe thunderstorm reports from across the CONUS were derived from the SPC

¹ All references to Fujita-scale damage ratings prior to 1 February 2007 are noted as being on the enhanced Fujita (EF) scale.

severe weather database, which originates from *Storm Data* reports collected by National Weather Service forecast offices and published by the National Climatic Data Center. The first database included all EF2 or greater tornadoes that were identified from January 2000 through December 2008. The second database consisted of all 2-in. (5.1 cm) or greater hail and 65-kt (33.4 m s^{-1} , where $1 \text{ kt} = 0.514 \text{ m s}^{-1}$) or greater wind reports (in the absence of tornadoes) from January 2003 through December 2008. The 9-yr database for significant tornadoes was chosen to ensure a similar sample size to the 6-yr database of significant wind and hail reports. We restricted our examination to significant severe reports because such events are more likely to be reported properly. Of course, any particular severe thunderstorm event is subject to the vagaries of damage ratings for tornadoes (Doswell and Burgess 1988) and the reporting system (e.g., Trapp et al. 2006), as well as potential errors in estimated magnitudes of wind and hail.

For each significant tornado event, the convective mode was determined at the beginning time of the report, utilizing base (0.5° -elevation angle) radar reflectivity mosaic images available from either the SPC severe thunderstorm events web page (<http://www.spc.noaa.gov/exper/archive/events/>), the image archive from the University Center for Atmospheric Research (<http://www.mmm.ucar.edu/imagearchive/>), or the Iowa Environmental Mesonet (<http://mesonet.agron.iastate.edu/GIS/apps/rview/warnings.phtml>). Three convective mode classifications were defined as follows:

- 1) *discrete cell*—relatively isolated cell(s) with a circular or elliptically shaped region of reflectivity with maximum values greater than or equal to 50 dBZ, after Trapp et al. (2005);
- 2) *QLCS*—a continuous major axis of at least 40-dBZ echoes with length greater than or equal to 100 km that shared a common leading edge and moved in tandem; additionally, the major axis had to be at least 3 times as long as the minor axis, following Trapp et al. (2005) and Grams et al. (2006); and
- 3) *cluster*—reserved for conglomerates of several cells that were not clearly identifiable as either discrete cell or QLCS in regional radar reflectivity mosaics, typically consisting of at least a contiguous region of 40-dBZ echoes in a 2500 km^2 (i.e., $50 \text{ km} \times 50 \text{ km}$) area.

The discrete cell and QLCS events were relatively easy to identify in most cases, as illustrated in Figs. 1a–c. Neither individual Weather Surveillance Radar-1988 Doppler (WSR-88D) site data, nor algorithm output, were utilized in the convective mode determination. Several of the cluster and QLCS categorizations may have consisted of more discrete or embedded supercell

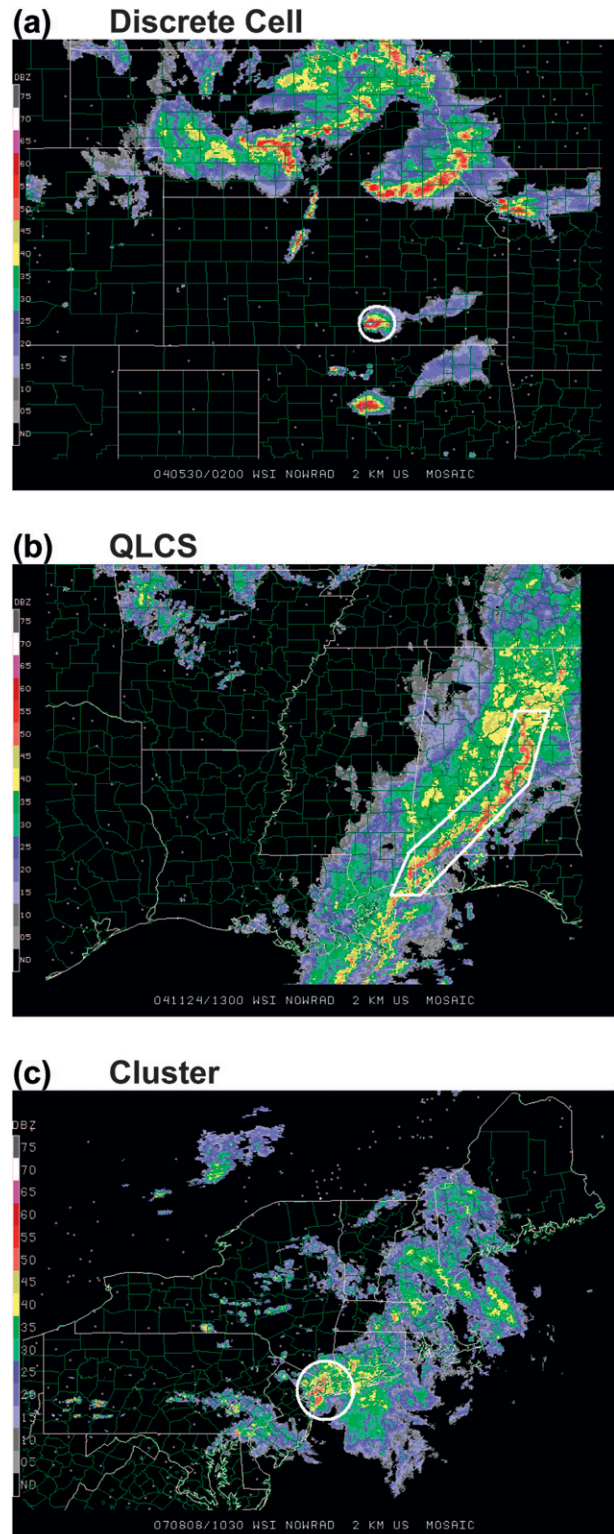


FIG. 1. Examples (highlighted by an oval or polygon) of convective modes derived from regional reflectivity mosaic images.

components when considering full-resolution (level II) reflectivity and velocity data. This is a distinct limitation of utilizing regional reflectivity mosaics because classification of supercell or nonsupercell archetypes is not possible. However, we believe that multiple subjective examinations (at least two and sometimes three independent classifications for each event) of the base reflectivity mosaic images were sufficient to correctly identify the basic radar reflectivity structures in the vast majority of events.

For each of the three convective modes, the most significant tornado damage rating was catalogued during each convective day (1200–1200 UTC), and these tornadoes served as the basis for subsequent data collection (if multiple tornadoes had the same damage rating, the earliest tornado was catalogued). Additional EF2 or greater tornadoes that occurred within 6 h and 300 km of the most significant tornado with each mode type were not considered as separate events. For example, multiple nearby significant tornadoes with multiple discrete cells were considered a single event in this sample. This approach reduced the chance that single outbreaks with many significant tornadoes would dominate the results and introduce data dependency into the sample. Similarly, the significant hail and wind databases were refined further to exclude events that occurred within 6 h and 300 km of any tornado, and only the largest hail and highest wind events of the convective day were catalogued.

b. Environmental data

Commonly utilized mandatory pressure-level and surface data were collected from two data sources. The primary source was the National Centers for Environmental Prediction (NCEP) operational Rapid Update Cycle (RUC) model (Benjamin et al. 2004) hourly analyses. For the initial time and location of a significant severe event, environmental conditions were assigned from the nearest analysis grid point at the closest hourly time. The 40-km (20 km) RUC model gridded analyses were utilized from May 2002 to December 2004 (from January 2005 to December 2008). It is acknowledged that this methodology for the spatiotemporal sampling of a severe storm environment may not necessarily be optimal (Potvin et al. 2010). However, these analyses were considered reasonable proxies for direct observations of the severe storm environment, following Thompson et al. (2003).

Prior to May 2002, archived RUC model analyses were unavailable. Thus, a secondary data source was a combination of station plots and automated 0000 and 1200 UTC mandatory pressure-level charts on the SPC

TABLE 1. Differences between subjectively interpolated mandatory pressure-level data and RUC model hourly analyses for 219 significant tornado events from May 2002 through December 2007.

500-hPa geopotential height		Mean difference: 9 m
Difference threshold (m)	No. of events	Percentage of events
±10	99	45%
±20	166	76%
±30	199	91%
500-hPa wind direction		Mean difference: -2.2°
Difference threshold (°)	No. of events	Percentage of events
±11.25	150	68%
±22.50	202	92%
700-hPa temperature		Mean difference: 0.0°C
Difference threshold (°C)	No. of events	Percentage of events
±1	173	79%
±2	210	96%
850-hPa dewpoint		Mean difference: 0.1°C
Difference threshold (°C)	No. of events	Percentage of events
±1	121	55%
±2	171	78%
±3	194	89%
850-hPa wind speed		Mean difference: -0.3 m s ⁻¹
Difference threshold (m s ⁻¹)	No. of events	Percentage of events
±2.5	110	50%
±5.0	186	85%
±7.5	204	93%

web page (<http://www.spc.noaa.gov/obs wx/maps/>). Mandatory pressure-level data were collected manually by temporally and spatially interpolating to the time and location of each significant tornado event. This dataset was used to form a comparison with the gridded RUC analysis data from May 2002 through December 2007. Differences between the two data retrieval methods were generally small with negligible biases (Table 1), further supporting our expectation of the RUC analysis being a reasonable approximation of the storm environment. Thus, the mandatory pressure-level data for the significant tornado event sample was composed of manually interpolated observed data from January 2000 to April 2002 for 104 events and nearest RUC model grid point analyses from May 2002 to December 2008 for the remaining 344 events.

Sounding-based parameter data were derived from the SPC severe storm environment database (Dean and Schneider 2008) from January 2003 (the beginning of the

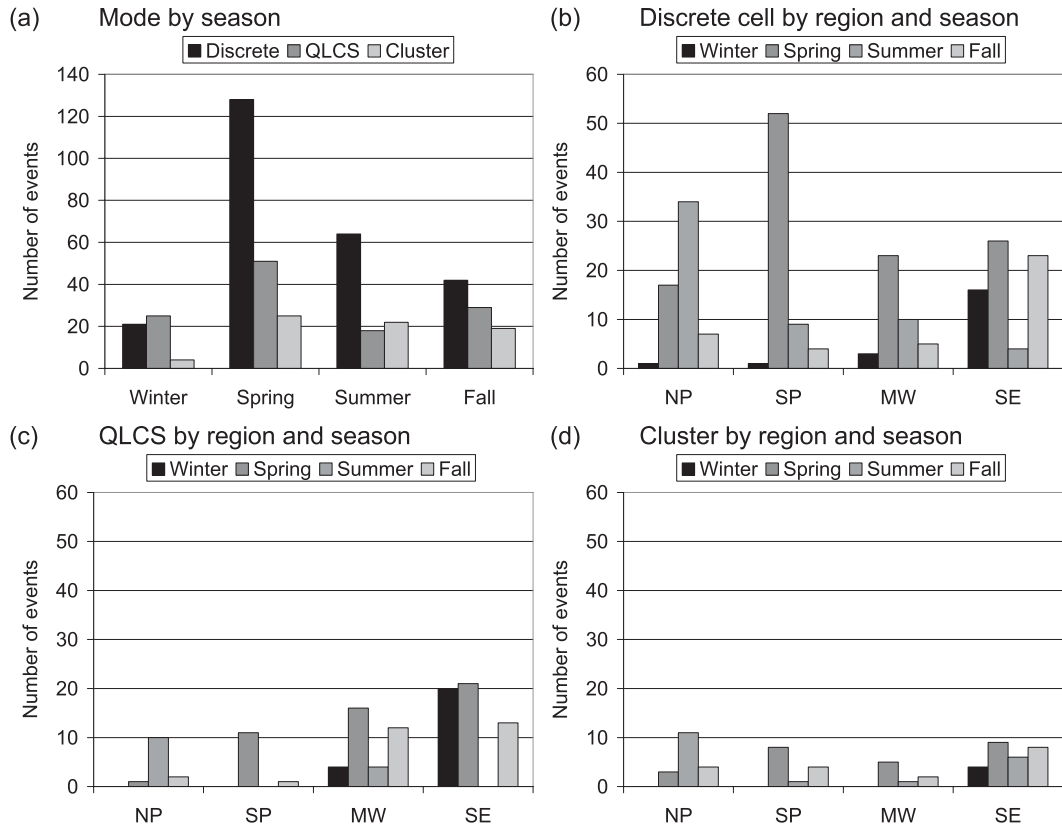


FIG. 4. Distribution by numbers of significant tornado events for (a) convective mode by season, (b) discrete cell, (c) QLCS, and (d) cluster modes by region (NP = northern plains; SP = southern plains; MW = Midwest; SE = Southeast) and season.

Significant tornado events were substantially less common across the western Great Plains from New Mexico to Montana, though lower population densities and fewer structures suggest that a larger percentage of tornadoes here may be underrated or underreported compared to areas farther east in the Great Plains and Mississippi River valley (e.g., Rasmussen 2003). Relatively few significant tornado events were documented from the central Appalachians into New England, along with the western United States. Regional subdivisions marked in Fig. 3 were based on geographic features (e.g., the Rockies and Appalachians) and climatological variations in seasonal flow regimes (e.g., oscillation of stronger prevailing westerlies from the southern Great Plains to the northern Great Plains, low-level wind direction and resultant moisture distributions from the southern plains to the Southeast).

Convective mode varied notably by season, with a clear majority of spring (March–May) and summer (June–August) significant tornado events associated with discrete cells (Fig. 4a). Significant tornado events with QLCSs also peaked in the spring, though at much lower frequencies compared to discrete cells. Significant tornado events with QLCSs varied by roughly a factor of 2.5

across all four seasons, compared to a factor of 6 for discrete cell events. The convective mode associated with significant tornadoes in the winter, when the frequencies of QLCS and discrete cell events were nearly identical, differed substantially from other seasons.

A further regional and seasonal breakdown of events reveals several important differences in convective mode and significant tornado occurrence. From Figs. 4b–d, it is seen that a vast majority of southern plains significant tornado events occurred with discrete cells during the spring, with a similar signal across the northern plains in the summer. Significant tornado events were also more common with discrete cells across the Midwest in the spring. QLCS significant tornado events occurred at nearly the same frequency in the Southeast in the spring and winter (December–February), and also displayed a moderate number of events in the fall. The relative maximum for discrete cell significant tornado events during the fall (September–November) in the Southeast was a result of the large number of tropical cyclone landfalls and associated tornadoes in 2004 and 2005 (Edwards 2010).

Marked differences were noted in the temporal distributions of significant tornadoes within the warm season

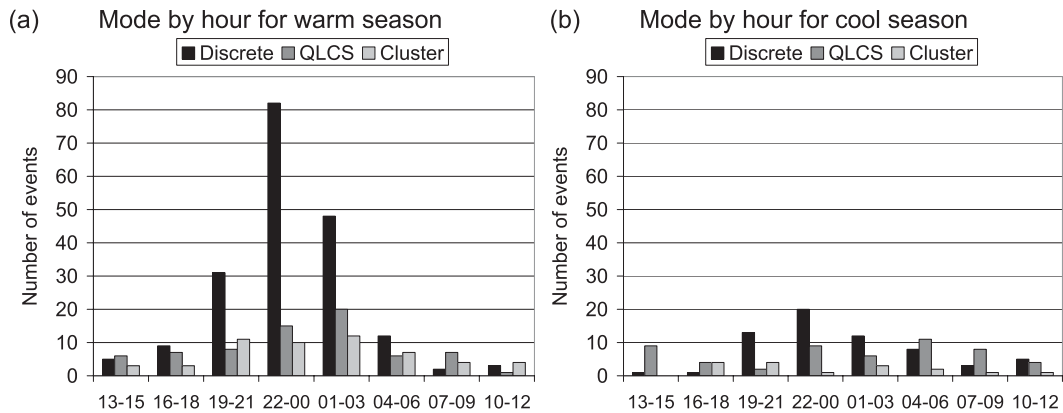


FIG. 5. Temporal distribution by numbers of significant tornado events for convective mode in 3-h bins (UTC) for the (a) warm and (b) the cool seasons.

(April–October; see Fig. 5a). All events were binned into 3-h periods to dampen sampling vagaries and maintain the more prominent signals in the data (similar to Trapp et al. 2005). The discrete cell events exhibited a pronounced diurnal cycle with a sharp peak in events near 0000 UTC. The QLCS and cluster significant tornado events displayed a similar diurnal maximum at a much lower magnitude. Interestingly, the number of QLCS significant tornado events (21) during the morning (from 0700 to 1800 UTC) was roughly equivalent to the number of discrete cell significant tornado events (19). Cool season events (November–March; see Fig. 5b) were substantially less frequent than during the warm season, and the diurnal peak in discrete cells was much less pronounced. The QLCS tornado events were more evenly distributed with relative maxima near 0600 and 1500 UTC, and an absolute minimum near 2100 UTC. This minimum in QLCS events near the peak of the diurnal heating cycle appears to be the most noteworthy difference compared to the discrete cell events, suggesting cool season QLCS significant tornado events are more synoptically driven.

b. Hail and wind events

A sample of 355 significant hail and 556 significant wind events was collected during the 6-yr period from January 2003 through December 2008 across the CONUS. These events were further subdivided into regions and seasons, requiring at least 24 or more separate tornado, hail, and wind events for convective mode and parameter comparisons (to be shown in sections 4 and 5). This requirement was only met in three regions and seasons: southern plains spring, Southeast spring, and the northern plains summer.

The relative frequency of convective mode in each region and season varied markedly for each severe weather type (Figs. 6a–c). Discrete cells dominated

Great Plains significant tornado events in the spring and summer, with a more even distribution in the Southeast spring compared to QLCS classifications. Significant hail–nontornado events were mostly discrete cells with a minimal number of QLCS classifications. Convective mode appeared to be more evenly distributed for significant wind–nontornado events. However, clusters and discrete cells represented a clear majority compared to QLCSs. Interestingly, the largest relative frequency of QLCS classifications was associated with significant tornadoes in the Southeast spring, and not with significant wind events that occurred in the absence of nearby tornadoes.

4. Parameter distributions

a. Winds and heights

Midlevel flow for the significant tornado sample was clustered around the southwest direction (225°) in the Southeast during fall and winter, compared to having a more westerly component in the spring (Fig. 7a). This tendency was also noted when compared to the three other region and season combinations. Fall events in the Southeast tended to have more southerly 850-hPa winds compared to spring and winter, a reflection of the influence of tropical cyclones during this period (Fig. 7b). Flow at 850 hPa was typically more southerly in the southern plains significant tornado events during spring compared to the Midwest and Southeast, and this tendency was noted in comparing Great Plains and Southeast events across the spectrum of severe events (not shown). In comparison to both significant hail and wind events occurring in the absence of tornadoes, significant tornado events had a statistically significant tendency for a more southwesterly versus westerly component to the flow at 500 hPa for the Southeast and southern plains spring and northern plains summer (not shown).

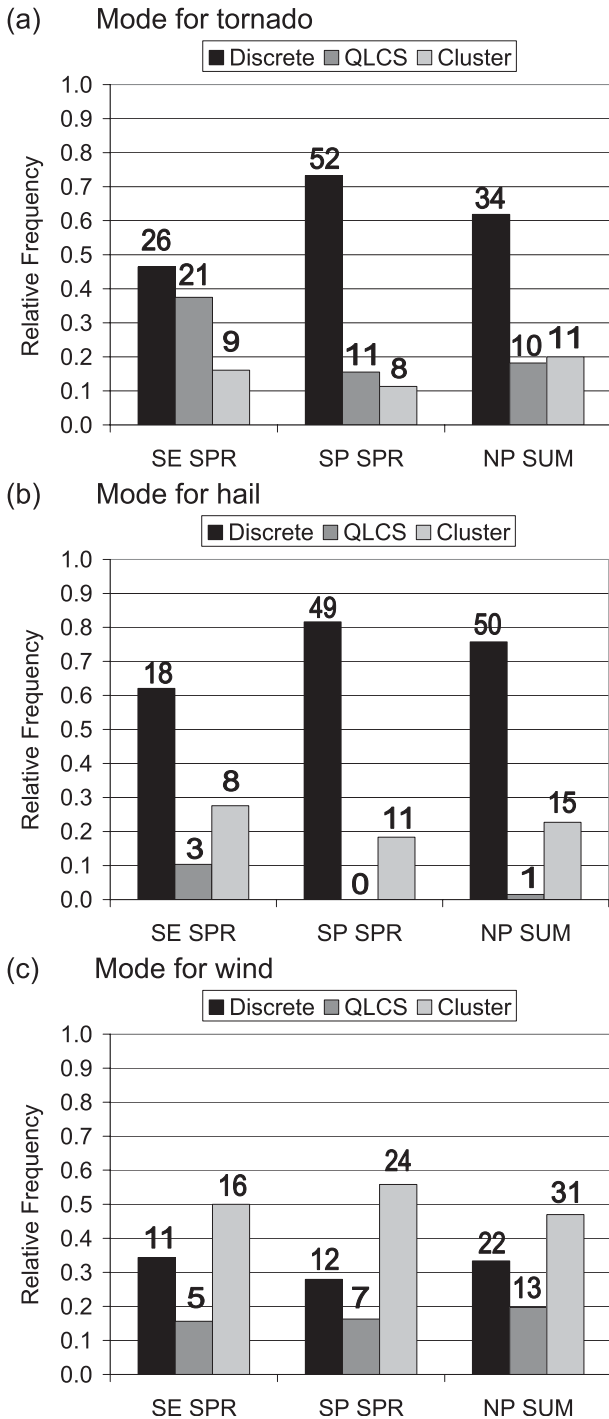


FIG. 6. Relative frequency of convective mode by type of significant severe event: (a) tornado, (b) hail, and (c) wind, for the Southeast spring (SE SPR), southern plains spring (SP SPR), and northern plains summer (NP SUM). The count of events is provided above each bar graph.

Figures 8a and 8b depict substantially weaker 500- and 850-hPa winds in northern plains summer significant tornado events compared to all other regions and

seasons. This corresponds to the annual oscillation in location and amplitude of the polar westerlies over the CONUS, and the relationship of the polar jet to the low-level jet in severe weather situations (e.g., Uccellini and Johnson 1979). Overall, wind speeds were generally lower in events across the Great Plains compared to the Southeast and Midwest. However, in comparison to Figs. 7a and 7b, a larger degree of veering of the wind profile can be inferred in events over the Great Plains, with greater magnitude difference in wind direction between 850 and 500 hPa. This suggests that both speed and direction play important roles in determining the magnitude of ground-relative vertical wind shear in the Great Plains; whereas more unidirectional and stronger kinematic profiles tend to characterize the Southeast and Midwest. Although this is a typical operational observation, it is not as directly relevant to storm dynamics when the traditional definitions of directional and speed shear are applied to storm-relative winds (Markowski and Richardson 2006).

Both 500- and 850-hPa wind speeds were substantially greater for significant tornado versus significant hail and wind events, with this differentiation most apparent in the Southeast spring (Figs. 9a and 9b). This is suggestive of a more amplified synoptic pattern or stronger mean flow during significant tornado days. This finding agrees with the proximity sounding work of Markowski et al. (2003), where significantly tornadic supercell events were characterized by stronger ground-relative winds compared to nontornadic supercell events.

The 500-hPa height falls (tornado time minus 12 h) for the significant tornado sample were most pronounced over the Southeast in winter, and smallest over the northern plains in summer (Fig. 10a). This similar trend was noted when comparing significant tornado events to the significant hail events (Fig. 10b) with a statistically significant tendency to have greater height falls in the Southeast and southern plains in spring with the tornado events. Interestingly, almost half of all significant tornado events were characterized by only small 500-hPa height falls (less than 30 m), or small height rises (especially during the northern plains summer). It should be noted that the height changes described here refer to the immediate vicinity of the significant severe events, while greater upstream height falls could occur in closer proximity to synoptic-scale troughs.

b. Temperature and dewpoint

The distribution of 500-hPa temperatures for the significant tornado sample in the Southeast fall is similar to (although broader than) the northern plains summer (Fig. 11a). The warmer 700-hPa temperatures over the northern plains (Fig. 11b) are consistent with steeper

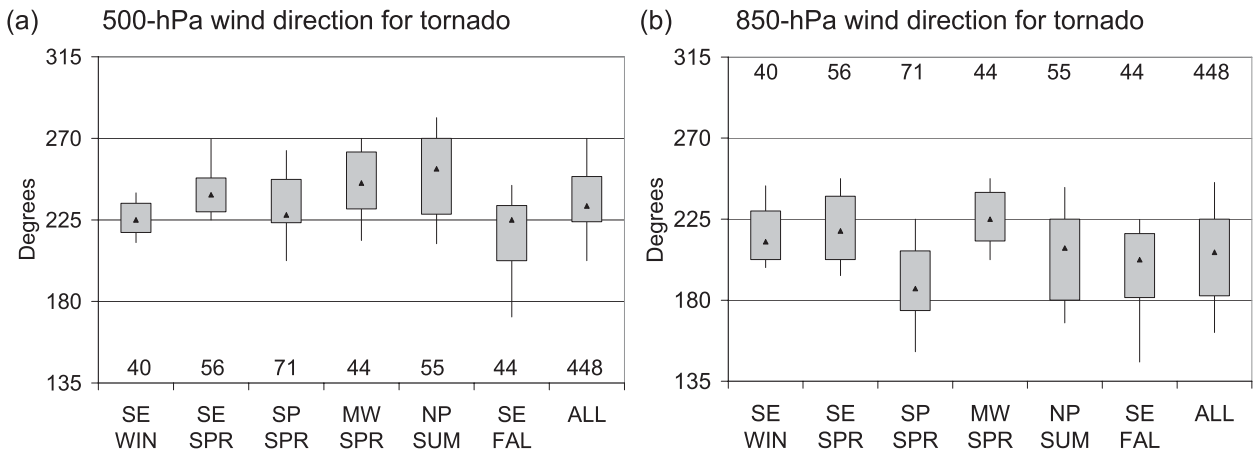


FIG. 7. Box-and-whiskers plots of (a) 500- and (b) 850-hPa wind direction ($^{\circ}$) for significant tornadoes in SE SPR, SP SPR, Midwest spring (MW SPR) NP SUM, Southeast fall (SE FAL), Southeast winter (SE WIN), and the entire sample (ALL). The shaded box covers the 25th–75th percentiles, the whiskers extend to the 10th and 90th percentiles, and the median values are marked by a triangle within each shaded box. The count of events is provided along the x axis.

midlevel temperature lapse rates in the northern plains summer compared to the Southeast fall (not shown). In the spring, southern plains 700-hPa temperatures are noticeably warmer than over the Midwest or Southeast (Fig. 11b), reflecting the EML source region over the Southwest (upstream from the Great Plains).

The mean 850-hPa dewpoints for the significant tornado sample were roughly 4°C greater across all regions and seasons than were found for a 6.5-yr dataset of both significant and nonsignificant tornadoes by David (1976). The greatest regional and seasonal differences are between the northern plains summer and Southeast winter (Fig. 11c). Despite these differences, the mean increase in 850-hPa dewpoint of 3.3°C from 12 h prior to initial tornado time was consistent across all regions and seasons (Fig. 12a). Figures 12b and 12c depict a roughly neutral thermal change at 500 hPa directly over the significant

tornado locations and only slight warming at 850 hPa, with relatively minor variations in the median noted among regions and seasons. This suggests that the local time tendency of moisture plays a larger role than temperature in the low levels for conditioning the thermodynamic environment prior to significant tornado events. This finding is important, since changes in lifted parcel moisture have approximately twice the impact on CAPE as temperature (e.g., Crook 1996).

Although the distribution of surface temperatures varies greatly based on season for the significant tornado sample (Fig. 13a), dewpoints depict less variation (Fig. 13b) with a mean of 66°F . The latter implies that although low-level moisture can be augmented by local sources, namely via evapotranspiration during the growing season (especially within the corn belt region of the Midwest and northern plains), the background synoptic regime is likely the

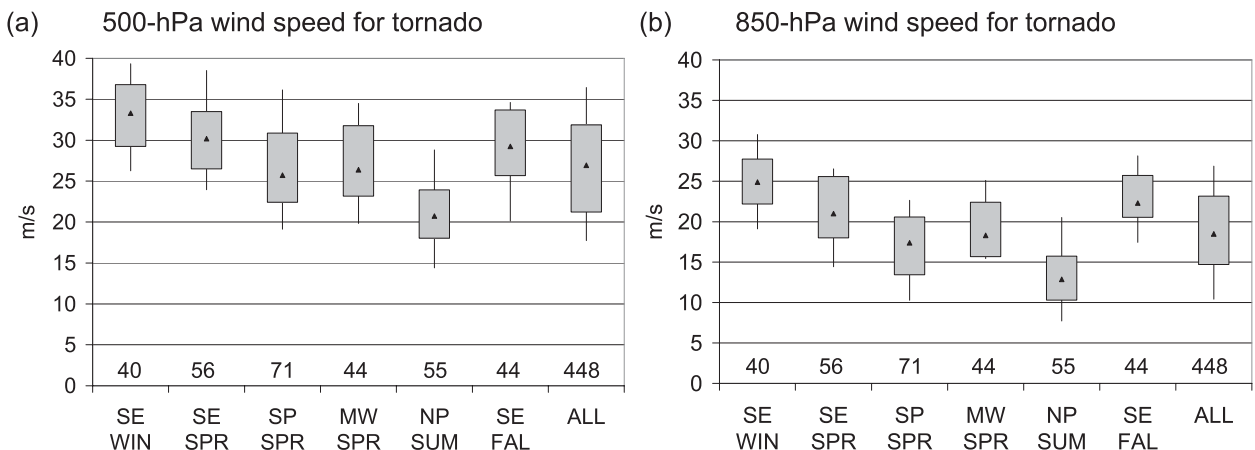


FIG. 8. As in Fig. 7, but for (a) 500- and (b) 850-hPa wind speeds (m s^{-1}).

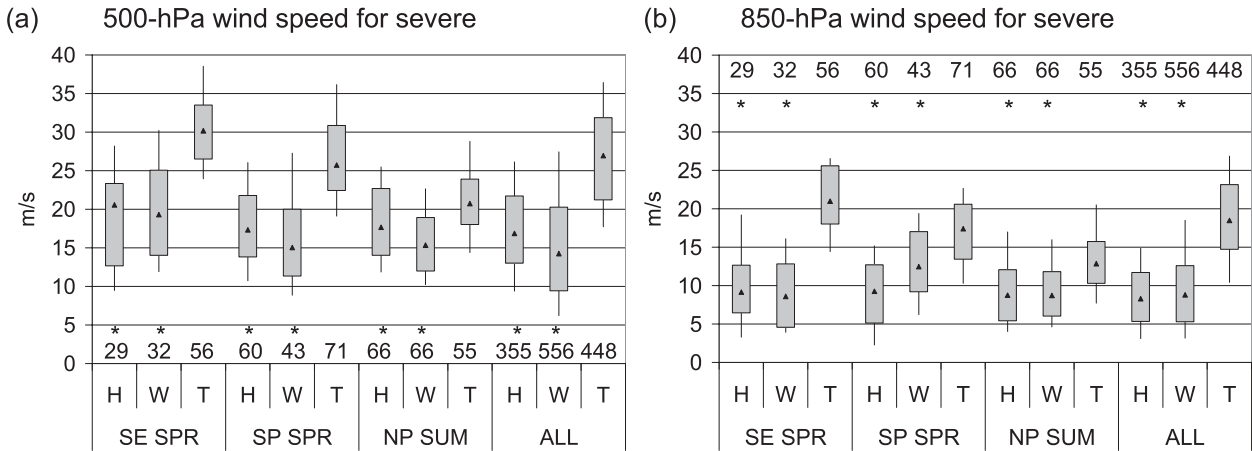


FIG. 9. As in Fig. 7, but for (a) 500- and (b) 850-hPa wind speeds ($m s^{-1}$) for significant severe events. An asterisk along the x axis indicates a statistically significant difference in the means between significant hail or wind events vs significant tornado events.

largest contributor to low-level moisture distributions through horizontal advection from a warm ocean source region (i.e., Gulf of Mexico).

c. Miller checklist comparison

A modified version of the Miller (1972) severe weather checklist (his Table 1, with categories of weak, moderate, and strong) utilizing percentile rank distributions is provided in Table 2, which lists only the variables included in our event sample. The median of our 90 significant tornado outbreak events (those representing six or more EF2+ tornadoes in a convective day) was consistent with Miller’s “strong” category for the magnitude of the low- and midtropospheric flow, low-level and surface dewpoint temperatures, as well as for surface pressure and 12-h pressure falls. Weaker winds in the “moderate” category characterized the upper-level

flow, along with low- and midtropospheric flow for 179 singular significant tornado events. Median 500-hPa 12-h height changes fell into Miller’s moderate category for our significant tornado outbreaks and into the “weak” category for the singular EF2 events. Operational forecasters sometimes focus on the more intense synoptic short-wave troughs and associated large midlevel height falls as an important component for forecasting significant tornado events. However, our relatively small 500-hPa height falls suggest this proxy for large-scale ascent need not be large directly over an area supportive of tornado development. This is consistent with the finding of weaker synoptic forcing (via upper-tropospheric potential vorticity advection) favoring discrete cell development (Schumann and Roebber 2010) and a greater threat for tornadoes (Thompson and Edwards 2000).

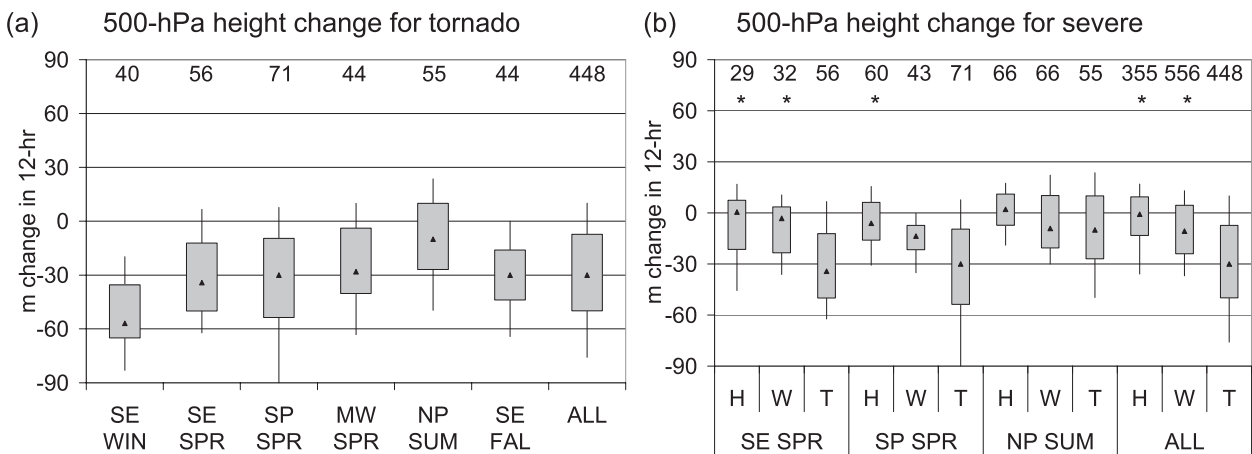


FIG. 10. As in Figs. 7 and 9, but for the 12-h change of geopotential height (m) at 500-hPa for (a) significant tornado and (b) significant severe events.

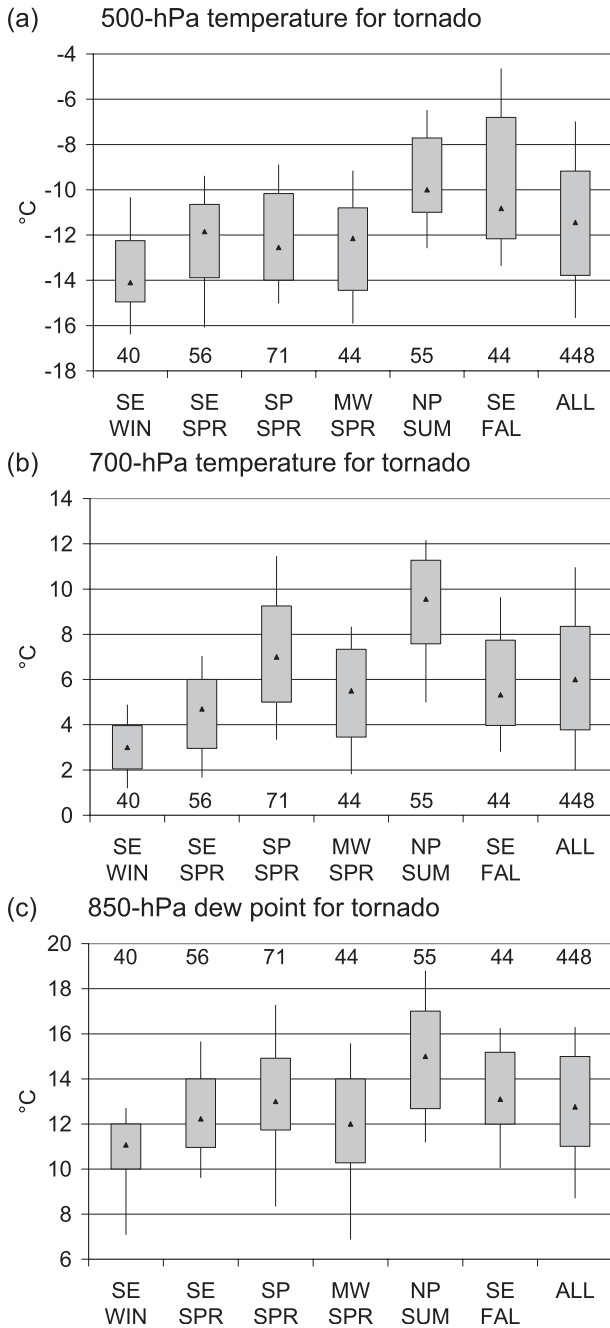


FIG. 11. As in Fig. 7, but for (a) 500- and (b) 700-hPa temperatures (°C), and (c) 850-hPa dewpoints (°C).

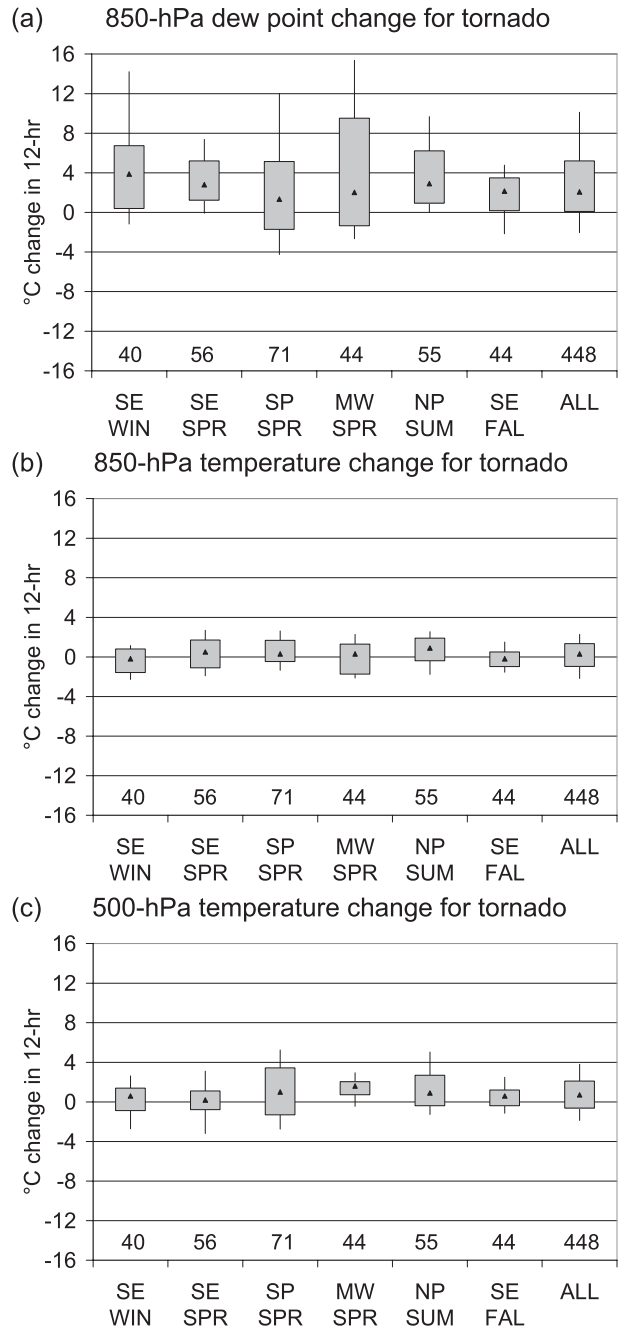


FIG. 12. As in Fig. 7, but for 12-h change of (a) 850-hPa dewpoints and (b) temperatures (°C), as well as (c) 500-hPa temperatures (°C).

d. Sounding-derived parameters

1) KINEMATIC VARIABLES

Figures 14a and 14b depict generally weaker bulk wind differences in northern plains summer events compared to all other regions and seasons, similar to the differences noted in 500- and 850-hPa wind speeds in section 4a. Low-level bulk wind differences tended to be weaker in Great

Plains environments compared to the Southeast and Midwest. Differences were more pronounced (and generally statistically significant) between significant tornado events versus significant hail and wind events (Figs. 15a and 15b). This was especially true for Southeast spring events where both low- and midlevel bulk wind differences were substantially greater for significant tornado events. These same trends were noted when comparing

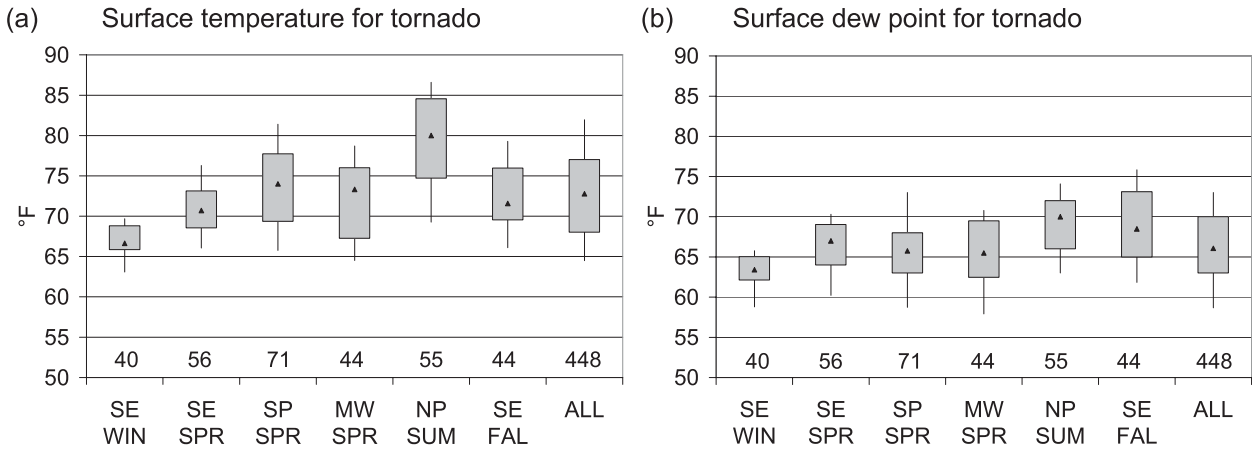


FIG. 13. As in Fig. 7, but for surface (a) temperatures (°F) and (b) dewpoints (°F).

effective bulk wind difference and storm-relative helicity (not shown).

2) THERMODYNAMIC VARIABLES

Great Plains and Midwest environments tended to be more unstable, with greater available buoyancy occurring over a larger distribution of values compared to events in the Southeast (Fig. 16a). Meanwhile, the median values of mixed layer convective inhibition (MLCIN) were generally similar across all regions and seasons (Fig. 16b). These same trends were also noted in most unstable CAPE and CIN comparisons (not shown). The mean mixed layer lifting condensation level (MLLCL) for the significant tornado events was 904 m, with overall distributions by region and season consistent with MLCAPE (Fig. 16c).

Overall differences in the distribution of MLCAPE appear to be modest between significant tornado versus significant hail and wind events (Fig. 17a). More prominent differences occurred with MLCIN and MLLCL, with a statistically significant tendency for weaker convective inhibition and lower LCL heights to accompany significant tornado events versus significant hail and wind

events in the northern plains summer (Figs. 17b and 17c). Though MLCAPE does not discriminate well between our classes of significant severe thunderstorm events, it is important to note that $MLCAPE > 500 \text{ J kg}^{-1}$ is necessary for the majority of the significant severe thunderstorm events.

3) COMPOSITE INDICES

Figure 18a shows that for all but Southeast winter, the 10th percentile of the supercell composite parameter (SCP) for each region and season was at or above 1, the approximate design threshold in the SCP for discrimination between supercell and nonsupercell discrete storms (Thompson et al. 2003). This infers that the majority of significant tornadoes in our sample occurred in environments favorable for discrete supercell storms (57% of the significant tornadoes in our sample were classified as discrete cell). Once again, the use of regional reflectivity mosaics limits the possibility of true classification based on supercell and nonsupercell archetypes. Substantial differences between significant tornado versus hail and wind events occur in the Southeast spring (Fig. 18b), with much higher values of SCP during significant tornado events.

TABLE 2. Percentile rank distributions of selected mandatory-level parameters for 90 events having days with at least six significant tornadoes (179 events having days with a single significant tornado in parentheses).

Parameter	Percentile				
	10th	25th	50th	75th	90th
300-hPa wind speed (kt)	42 (34)	59 (44)	70 (59)	82 (74)	96 (89)
500-hPa wind speed (kt)	44 (31)	49 (37)	60 (49)	70 (58)	75 (67)
850-hPa wind speed (kt)	30 (20)	35 (26)	44 (33)	50 (42)	60 (50)
850-hPa dewpoint (°C)	10 (8)	11 (11)	13 (13)	15 (15)	16 (16)
12-h surface pressure falls (hPa)	0 (1)	2 (2)	5 (5)	7 (7)	10 (9)
12-h 500-hPa height falls (m)	0 (-10)	18 (5)	35 (22)	60 (43)	71 (76)
Mean sea level pressure (hPa)	1008 (1011)	1006 (1009)	1004 (1006)	999 (1002)	996 (997)
Surface dewpoint (°F)	59 (58)	63 (63)	66 (66)	70 (70)	73 (73)

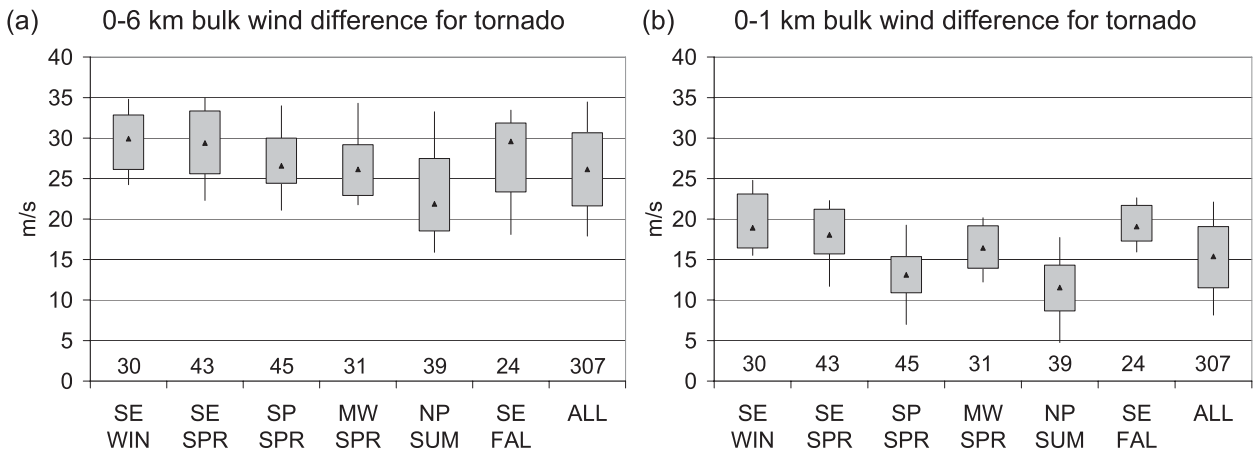


FIG. 14. As in Fig. 7, but for bulk wind differences ($m s^{-1}$) at (a) 0–6 and (b) 0–1 km.

This trend appears to a lesser extent (but still statistically significant) for southern plains spring and northern plains summer events.

The mean significant tornado parameter (STP) for the significant tornado events was 2.2. Figure 19a shows that for all but the Southeast winter, the 50th percentile was at or above 1, the approximate threshold that the STP was designed to discriminate between significant and nonsignificant tornadoes (Thompson et al. 2003). STP values were larger for significant tornado versus significant hail and wind events, and these differences were statistically significant for all three region and season combinations (Fig. 19b).

5. Comparison of discriminating factors for diagnostic utility

Following Rasmussen and Blanchard (1998) and Rasmussen (2003), Heidke’s skill score (HSS) was used

to assess the relative diagnostic accuracy of various environmental parameters in conjunction with convective mode, to provide an objective comparison of discrimination. Doswell et al. (1990) demonstrated that the HSS was superior to the critical success index (CSI) for evaluating forecasts of rare events because it gave credit for a correct forecast of a nonevent. To examine the ability of a parameter to diagnose the occurrence of significant tornadoes versus significant hail (in the absence of tornadoes) and significant tornadoes versus significant wind (in the absence of tornadoes), the following rule was used: given that a parameter is associated with the occurrence of a significant tornado, hail, or wind event, if the value of the parameter is greater than x , then a significant tornado will be associated with the parameter. Exceptions to this rule included MLLCL, 500-hPa height change, 500- and 850-hPa wind direction, and 700-hPa temperature where the value of the parameter was less than x . The value of x that maximized the HSS for this rule was sought, by

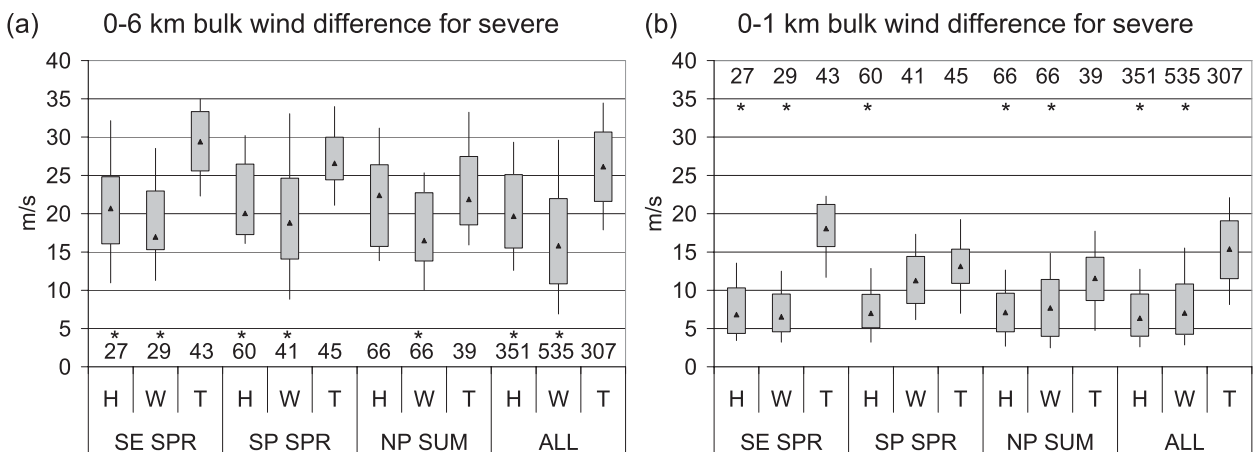


FIG. 15. As in Fig. 9, but for bulk wind difference ($m s^{-1}$) at (a) 0–6 and (b) 0–1 km.

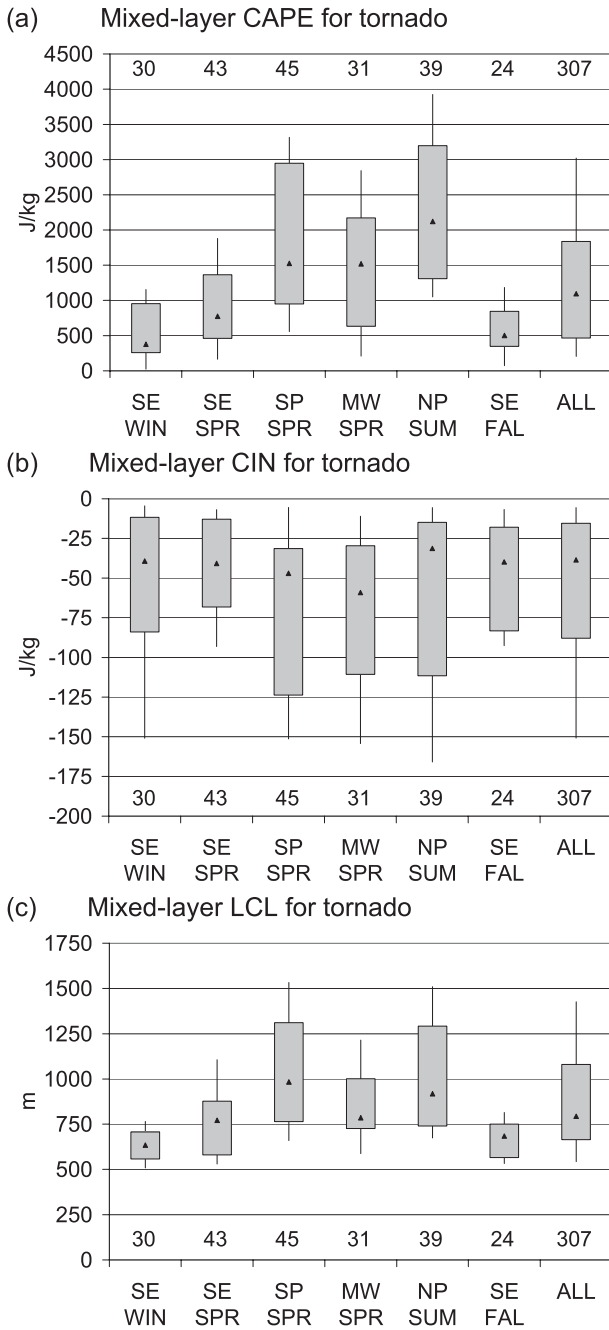


FIG. 16. As in Fig. 7, but for ML (a) CAPE ($J\ kg^{-1}$), (b) CIN ($J\ kg^{-1}$), and (c) LCL (m).

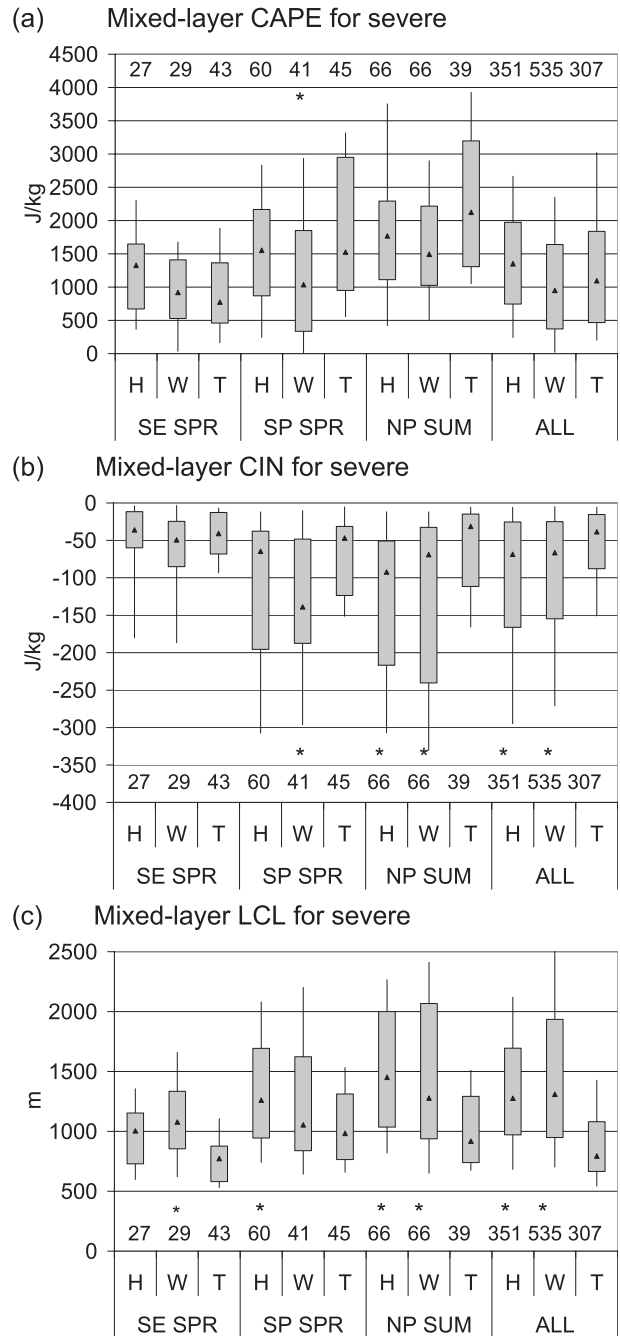


FIG. 17. As in Fig. 9, but for ML (a) CAPE ($J\ kg^{-1}$), (b) CIN ($J\ kg^{-1}$), and (c) LCL (m).

examining HSS for all possible x_s . For convective mode discrimination, categorical occurrence or nonoccurrence was assigned for each type prior to HSS calculation.

Table 3 depicts the HSS for 19 tested parameters with significant tornado versus significant hail and wind events (in the absence of tornadoes), both individually and for the combination of the Southeast spring, southern plains spring, and northern plains summer. Several similarities

and differences can be gleaned from Table 3, which depicts the 10 highest HSSs within each column. Given the observational experience that most significant tornado and hail events are commonly associated with supercells, the importance of low- and midlevel winds to discriminate between these types of significant severe events could largely be expected. This is supported by the

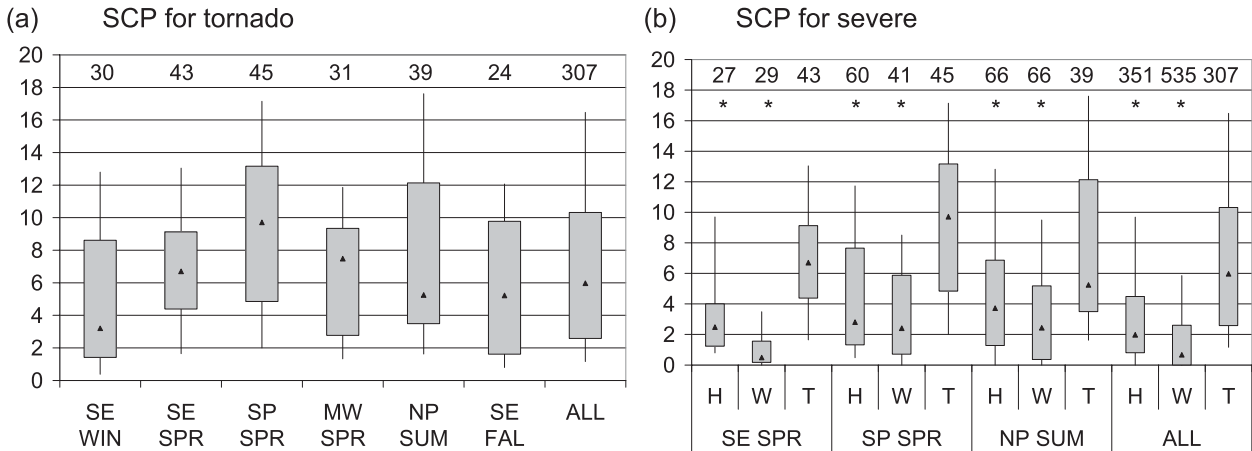


FIG. 18. As in Figs. 7 and 9, but for the SCP for (a) significant tornado and (b) significant severe events.

finding of Markowski et al. (2003) that ground-relative wind speeds are larger in significant tornado environments than in weak tornado and nontornado environments, and that this result was more statistically robust in the low- to midtroposphere. As noted in section 3b, a near-complete lack of significant hail–nontornado events associated with QLCS convective mode (2%) is supported by an HSS of 0.278 for the occurrence of significant tornadoes with QLCS convective mode.

Similar to the significant hail event comparison, the stronger the low- and midlevel winds, the greater the likelihood for significant tornado events versus significant wind–nontornado events. The relatively high ranking of cluster (HSS of 0.417) and discrete cell (HSS of 0.330) convective modes underlies the value of convective mode when attempting to discriminate between significant tornado and significant wind–nontornado events.

Overall, the relatively greater importance of composite and kinematic parameters can be seen compared

to thermodynamic parameters. This is consistent with the finding from Shafer et al. (2010) that storm-relative helicity parameters provided greater discrimination between Weather Research and Forecasting Model (WRF) estimates of tornado outbreaks and primarily non-tornadic outbreaks, compared to CAPE. Nevertheless, certain thermodynamic parameters can provide relatively high levels of discrimination in specific regions and seasons (e.g., MLLCL in the Southeast spring and northern plains summer for significant tornado versus both significant hail and wind events). This suggests that given an a priori expectation of a significant severe event, composite and kinematic parameters, along with convective mode, should play more prominent roles in anticipating the type of significant severe events. This does not imply that thermodynamic parameters are unimportant; rather, their importance is likely larger when comparing a significant tornado event and a true null-tornado environment where significant severe storms did not occur.

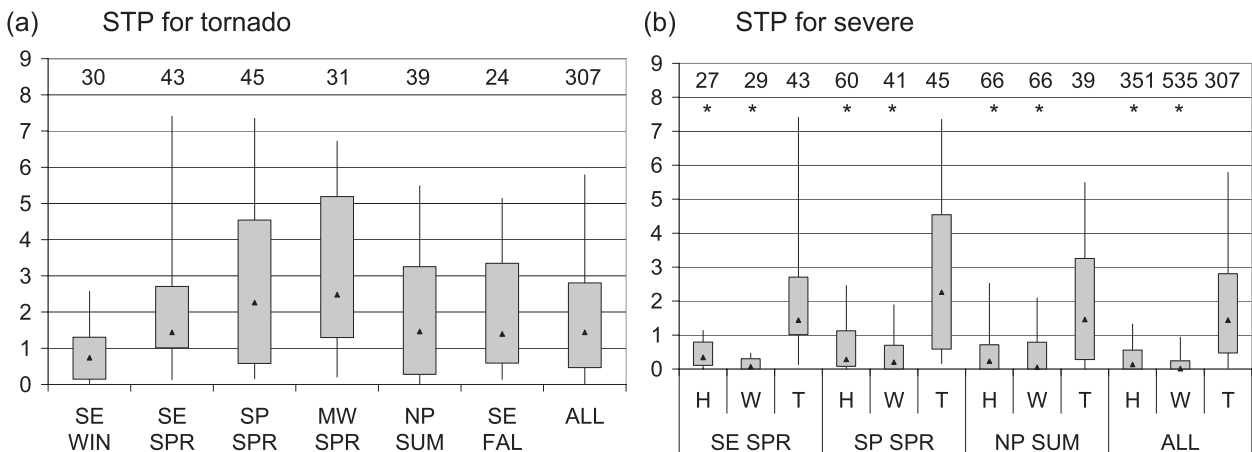


FIG. 19. As in Figs. 7 and 9, but for the STP for (a) significant tornado and (b) significant severe events.

TABLE 3. HSSs for selected parameters in the significant tornado vs significant hail–no tornado and significant wind–no tornado forecasts. The 10 highest HSSs for each column are displayed for SE SPR, SP SPR, and NP SUM, individually and combined.

Wind parameter	Hail				Wind			
	SE SPR	SP SPR	NP SUM	Total	SE SPR	SP SPR	NP SUM	Total
Cluster mode	—	—	—	—	0.375	0.494	0.305	0.417
Discrete mode	—	—	—	—	—	0.455	0.283	0.330
QLCS mode	0.305	—	0.255	0.278	—	—	—	—
STP	0.602	0.443	0.440	0.472	0.727	0.476	0.391	0.496
SCP	0.534	0.407	—	0.339	0.681	0.471	0.380	0.453
0–1-km bulk wind difference	0.810	0.550	0.382	0.555	0.815	—	0.336	0.412
850-hPa wind speed	0.773	0.629	0.372	0.588	0.754	0.338	0.355	0.489
850-hPa wind direction	—	—	—	—	0.442	—	—	—
0–6-km bulk wind difference	0.539	0.409	—	0.308	0.619	0.527	0.322	0.486
500-hPa wind speed	0.652	0.541	0.283	0.441	0.657	0.657	0.425	0.557
500-hPa wind direction	0.448	0.471	0.389	0.423	—	0.395	—	0.325
12-h 500-hPa height change	0.439	0.481	0.329	0.410	0.439	0.362	—	0.327
MLCAPE	—	0.327	—	—	—	—	0.337	—
MLCIN	—	—	0.354	—	—	0.321	—	—
MLLCL	0.353	—	0.391	0.349	0.506	—	0.301	—
Surface dewpoint	—	0.299	0.367	—	—	—	—	—
850-hPa dewpoint	—	—	—	—	—	—	—	—
Surface temp	—	—	—	—	—	—	—	—
700-hPa temp	—	—	—	—	—	—	—	—

In addition, it is important to note that some of the mandatory-level variables actually discriminate similar to or better than their corresponding sounding-derived measures for significant tornado events versus significant severe–nontornado events (e.g., 500- and 850-hPa wind speeds versus 0–6- and 0–1-km bulk wind differences). This appears to be especially true for kinematic parameters and infers that it may largely remain a matter of preference over whether a forecaster should use a base-state display of wind speeds or sounding-derived calculated wind shear when attempting to forecast a significant tornado environment compared to a significant severe–nontornado environment.

6. Summary and discussion

A sample of 448 significant tornado (EF2 + damage) events and associated convective mode was collected for the 9-yr period from January 2000 through December 2008, based on *Storm Data* reports and regional radar reflectivity mosaic images. Significant tornadoes were most common with discrete cells (57% of events, 69% of total tornadoes), while QLCSs accounted for 27% of our events (20% of total tornadoes), and clusters contained the remaining 16% of our events (11% of total tornadoes). Significant tornadoes occurred most frequently with discrete cells in the spring (southern plains) and summer (northern plains), while QLCS significant tornadoes were more evenly distributed throughout the year. Significant tornadoes occurred at nearly equal frequencies

with discrete cells and QLCSs in the Southeast during the winter and spring. The discrete cell events displayed a clear diurnal peak near 0000 UTC and a minimum during the overnight/morning hours. A muted peak in QLCS tornadoes was noted around 0000 UTC during the warm season, with more evenly distributed occurrences at various times of day during the cool season. This suggests that the most difficult tornado forecasts associated with convective mode are during the winter in the Southeast, while significant tornadoes occur most consistently with discrete cells across the southern plains in the spring and northern plains in the summer during the late afternoon to early evening.

We have largely replicated the results of prior studies that focused on mandatory pressure-level data (e.g., Miller 1972; David 1976), with a few noteworthy exceptions. Temperature changes aloft (e.g., 500 hPa) were rather small in the 12-h period leading up to the significant tornado events, but local moistening of roughly 2°–4°C at 850 hPa was documented. Somewhat surprisingly, 12-h 500-hPa height falls were typically only around 30 m in the immediate area of the significant tornado events. Owing in part to the previous studies from the 1970s, operational forecasters sometimes tend to focus on the more intense and rapidly moving synoptic systems, with larger resultant change fields, when attempting to forecast significant tornado episodes. The synoptic systems associated with significant tornado events vary from barely perceptible to high-amplitude waves, but the degree of large-scale ascent inferred solely from midlevel

height falls need not be large in magnitude directly over the location of a significant tornado. Even so, greater midlevel height falls do tend to characterize significant tornado environments compared to significant hail and wind events in the absence of tornadoes.

An objective measure (HSS) of discrimination between significant tornadoes and significant hail and wind events in the absence of tornadoes was provided for diagnostic utility. This helps synthesize the key considerations for forecasting such events by showing the relative discriminating power between mandatory pressure-level data, sounding-based derived parameters, and convective mode, all of which are routinely produced by model guidance available within the operational community. Relatively greater discrimination occurs between composite parameters, kinematic variables (whether mandatory pressure level or sounding derived), and convective mode compared with thermodynamic variables. Given a forecaster's conditional anticipation of a significant severe event, the magnitude of low- and midlevel ground-relative wind speeds in combination with composite parameters and the type of convective mode should largely aid the forecaster with the expected type of severe event. The success of pattern recognition in significant tornado forecasting is largely a function of how consistently the identified pattern relates to the generation and collocation of the necessary ingredients for tornadic supercells, which account for the largest percentage of significant tornado events and outbreaks.

Work is on going to expand upon the comparison of convective mode to kinematic and thermodynamic parameters for a broad spectrum of severe weather events, with the development of a comprehensive database of radar-based convective morphology for all tornado, along with all significant hail and wind events in the CONUS since 2003. Classification of convective mode is being performed with full-resolution reflectivity and velocity data from an individual WSR-88D closest to a given report. This allows for the determination of supercell versus nonsupercell storms, and should lead to more precise classifications with higher temporal and spatial resolutions than regional reflectivity mosaics (see Smith et al. 2010; Thompson et al. 2010).

Acknowledgments. The authors thank Adam Cale with Iowa State University for producing independent convective mode classifications for a portion of the significant hail and wind events, Andrew Dean (SPC) for providing sounding-based environmental data for most of the severe events, Heather Grams with the University of Oklahoma for her assistance in creating scripts to decode RUC grib files and extract point data for individual events, and Steven Weiss (SPC) for discussions regarding

this project. Finally, this paper was greatly improved by thorough reviews from Matthew Bunkers of NWS Rapid City, James Correia Jr. (SPC), and one anonymous reviewer.

REFERENCES

- Benjamin, S. G., and Coauthors, 2004: An hourly assimilation-forecast cycle: The RUC. *Mon. Wea. Rev.*, **132**, 495–518.
- Bluestein, H. B., 1999: A history of severe-storm-intercept field programs. *Wea. Forecasting*, **14**, 558–577.
- Bothwell, P. D., J. A. Hart, and R. L. Thompson, 2002: An integrated three-dimensional objective analysis scheme in use at the Storm Prediction Center. Preprints, *21st Conf. on Severe Local Storms/19th Conf. on Weather Analysis and Forecasting/15th Conf. on Numerical Weather Prediction*, San Antonio, TX, Amer. Meteor. Soc., JP3.1. [Available online at <http://ams.confex.com/ams/pdfpapers/47482.htm>.]
- Bunkers, M. J., J. S. Johnson, L. J. Czepyha, J. M. Grzywacz, B. A. Klimowski, and M. R. Hjelmfelt, 2006: An observational examination of long-lived supercells. Part II: Environmental conditions and forecasting. *Wea. Forecasting*, **21**, 689–714.
- , J. R. Wetenkamp Jr., J. J. Schild, and A. Fischer, 2010: Observations of the relationship between 700-mb temperatures and severe weather reports across the contiguous United States. *Wea. Forecasting*, **25**, 799–814.
- Corfidi, S. F., 1999: The birth and early years of the Storm Prediction Center. *Wea. Forecasting*, **14**, 507–525.
- Crook, N. A., 1996: Sensitivity of moist convection forced by boundary layer processes to low-level thermodynamic fields. *Mon. Wea. Rev.*, **124**, 1767–1785.
- David, C. L., 1976: A study of upper air parameters at the time of tornadoes. *Mon. Wea. Rev.*, **104**, 546–551.
- Davies-Jones, R., R. J. Trapp, and H. B. Bluestein, 2001: Tornadoes and tornadic storms. *Severe Convective Storms, Meteor. Monogr.*, No. 50, Amer. Meteor. Soc., 167–222.
- Dean, A. R., and R. S. Schneider, 2008: Forecast challenges at the NWS Storm Prediction Center relating to the frequency of favorable severe storm environments. Preprints, *24th Conf. on Severe Local Storms*, Savannah, GA, Amer. Meteor. Soc., 9A.2. [Available online at <http://ams.confex.com/ams/pdfpapers/141743.htm>.]
- Dial, G. L., J. P. Racy, and R. L. Thompson, 2010: Short-term convective mode evolution along synoptic boundaries. *Wea. Forecasting*, **25**, 1430–1446.
- Doswell, C. A., III, and D. W. Burgess, 1988: Some issues of United States tornado climatology. *Mon. Wea. Rev.*, **116**, 495–501.
- , R. Davies-Jones, and D. L. Keller, 1990: On summary measures of skill in rare event forecasting based on contingency tables. *Wea. Forecasting*, **5**, 576–585.
- , H. E. Brooks, and R. A. Maddox, 1996: Flash flood forecasting: An ingredients-based methodology. *Wea. Forecasting*, **11**, 560–581.
- Duda, J. D., and W. A. Gallus Jr., 2010: Spring and summer midwestern severe weather reports in supercells compared to other morphologies. *Wea. Forecasting*, **25**, 190–206.
- Edwards, R., 2010: Tropical cyclone tornado records for the modernized NWS era. Preprints, *25th Conf. on Severe Local Storms*, Denver, CO, Amer. Meteor. Soc., P3.1. [Available online at <http://ams.confex.com/ams/pdfpapers/175269.htm>.]
- Gallus, W. A., Jr., N. A. Snook, and E. V. Johnson, 2008: Spring and summer severe weather reports over the Midwest as a

- function of convective mode: A preliminary study. *Wea. Forecasting*, **23**, 101–113.
- Galway, J. G., 1992: Early severe thunderstorm forecasting and research by the United States Weather Bureau. *Wea. Forecasting*, **7**, 564–587.
- Grams, J. S., W. A. Gallus Jr., S. E. Koch, L. S. Wharton, A. Lough, and E. E. Ebert, 2006: The use of a modified Ebert–McBride technique to evaluate mesoscale model QPF as a function of convective system morphology during IHOP 2002. *Wea. Forecasting*, **21**, 288–306.
- Hart, J. A., and W. D. Korotky, 1991: The SHARP workstation v1.50 users guide. NOAA/NWS, 30 pp. [Available from NWS Eastern Region Headquarters, 630 Johnson Ave., Bohemia, NY 11716.]
- Johns, R. H., and C. A. Doswell III, 1992: Severe local storms forecasting. *Wea. Forecasting*, **7**, 588–612.
- , J. M. Davies, and P. M. Leftwich, 1993: Some wind and instability parameters associated with strong and violent tornadoes. Part II: Variations in the combinations of wind and instability parameters. *The Tornado: Its Structure, Dynamics, Hazards, and Prediction, Geophys. Monogr.*, Vol. 79, Amer. Geophys. Union, 583–590.
- Kain, J. S., M. E. Baldwin, P. R. Janish, S. J. Weiss, M. P. Kay, and G. W. Carbin, 2003: Subjective verification of numerical models as a component of a broader interaction between research and operations. *Wea. Forecasting*, **18**, 847–860.
- , and Coauthors, 2008: Severe-weather forecast guidance from the first generation of large-domain convection-allowing models: Challenges and opportunities. Preprints, *24th Conf. on Severe Local Storms*, Savannah, GA, Amer. Meteor. Soc., 12.1. [Available online at <http://ams.confex.com/ams/pdfpapers/141723.htm>.]
- Mann, H. B., and D. R. Whitney, 1947: On a test of whether one of two random variables is stochastically larger than the other. *Ann. Math. Stat.*, **18**, 50–60.
- Markowski, P., and Y. Richardson, 2006: On the classification of vertical wind shear as directional shear versus speed shear. *Wea. Forecasting*, **21**, 242–247.
- , C. Hannon, J. Frame, E. Lancaster, A. Pietrycha, R. Edwards, and R. L. Thompson, 2003: Characteristics of vertical wind profiles near supercells obtained from the Rapid Update Cycle. *Wea. Forecasting*, **18**, 1262–1272.
- Miller, R. C., 1972: Notes on analysis and severe-storm forecasting procedures of the Air Force Global Weather Central. Air Weather Service Tech. Rep. 200 (Rev.), Scott Air Force Base, 190 pp.
- Moller, A. R., 2001: Severe local storms forecasting. *Severe Convective Storms, Meteor. Monogr.*, No. 50, Amer. Meteor. Soc., 433–480.
- Potvin, C. K., K. L. Elmore, and S. J. Weiss, 2010: Assessing the impacts of proximity sounding criteria on the climatology of significant tornado environments. *Wea. Forecasting*, **25**, 921–930.
- Rasmussen, E. N., 2003: Refined supercell and tornado forecast parameters. *Wea. Forecasting*, **18**, 530–535.
- , and D. O. Blanchard, 1998: A baseline climatology of sounding-derived supercell and tornado forecast parameters. *Wea. Forecasting*, **13**, 1148–1164.
- Schaefer, J. T., 1986: Severe thunderstorm forecasting: A historical perspective. *Wea. Forecasting*, **1**, 164–189.
- Schumann, M. R., and P. J. Roebber, 2010: The influence of upper-tropospheric potential vorticity on convective morphology. *Mon. Wea. Rev.*, **138**, 463–474.
- Shafer, C. M., A. E. Mercer, L. M. Leslie, M. B. Richman, and C. A. Doswell III, 2010: Evaluation of WRF model simulations of tornadic and nontornadic outbreaks occurring in the spring and fall. *Mon. Wea. Rev.*, **138**, 4098–4119.
- Smith, B. T., R. L. Thompson, J. S. Grams, and C. Broyles, 2010: Climatology of convective modes for significant severe thunderstorms in the contiguous United States. Preprints, *25th Conf. on Severe Local Storms*, Denver, CO, Amer. Meteor. Soc., P2.7. [Available online at <http://ams.confex.com/ams/pdfpapers/175726.htm>.]
- Thompson, R. L., and R. Edwards, 2000: An overview of environmental conditions and forecast implications of the 3 May 1999 tornado outbreak. *Wea. Forecasting*, **15**, 682–699.
- , and C. M. Mead, 2006: Tornado failure modes in central and southern Great Plains severe thunderstorm episodes. Preprints, *23rd Conf. on Severe Local Storms*, St. Louis, MO, Amer. Meteor. Soc., 3.2. [Available online at <http://ams.confex.com/ams/pdfpapers/115239.htm>.]
- , R. Edwards, J. A. Hart, K. L. Elmore, and P. Markowski, 2003: Close proximity soundings within supercell environments obtained from the Rapid Update Cycle. *Wea. Forecasting*, **18**, 1243–1261.
- , B. T. Smith, J. S. Grams, A. R. Dean, and C. Broyles, 2010: Climatology of near-storm environments with convective modes for significant severe thunderstorms in the contiguous United States. Preprints, *25th Conf. on Severe Local Storms*, Savannah, GA, Amer. Meteor. Soc., 16B.6. [Available online at <http://ams.confex.com/ams/pdfpapers/175727.htm>.]
- Trapp, R. J., S. A. Tessendorf, E. S. Godfrey, and H. E. Brooks, 2005: Tornadoes from squall lines and bow echoes. Part I: Climatological distribution. *Wea. Forecasting*, **20**, 23–33.
- , D. M. Wheatley, N. T. Atkins, R. W. Przybylinski, and R. Wolf, 2006: Buyer beware: Some words of caution on the use of severe wind reports in postevent assessment and research. *Wea. Forecasting*, **21**, 408–415.
- Uccellini, L. W., and D. R. Johnson, 1979: The coupling of upper and lower tropospheric jet streaks and implications for the development of severe convective storms. *Mon. Wea. Rev.*, **107**, 682–703.
- Wilhelmson, R. B., and L. J. Wicker, 2001: Numerical modeling of severe local storms. *Severe Convective Storms, Meteor. Monogr.*, No. 50, Amer. Meteor. Soc., 123–166.